

Chemical characterization of the Neogene Aquifer, Belgium

Marleen Coetsiers · Kristine Walraevens

Abstract The evolution of groundwater chemistry along the direction of groundwater flow was studied using hydrochemical data from samples collected along a flow line in the Neogene Aquifer, Belgium. Infiltrating water was found to have a very low mineral content and low pH because the sediments are strongly decalcified. Increasing SiO₂ and cation concentrations along the groundwater flow line indicate silicate-weathering processes, confirmed with the aid of saturation indices, calculated with PHREEQC, and stability diagrams. A classification system based on redox sensitive species was developed and shows that an extensive redox sequence is present in the aquifer. At a shallow depth, pyrite oxidation has caused an increase in sulphate, while iron is precipitated as hydroxides. Elevated arsenic concentrations are related to the reduction of these iron hydroxides at a relatively shallow depth and to the dissolution of siderite at greater depth. Dissolution of carbonate in the aquifer material, present in deep layers and to the north, has lead to increased Ca²⁺ and HCO₃⁻ concentrations. The Ca²⁺ from the groundwater is exchanged for Na⁺, Mg²⁺ and K⁺ adsorbed to the clay surfaces at the bottom of the groundwater reservoir. Although the Neogene Aquifer is well flushed, there are still some marine influences present in the deepest parts.

Résumé L'évolution de la chimie des eaux souterraines le long des directions d'écoulement a été étudiée à partir données hydrochimiques issues de prélèvements effectués le long d'une ligne de flux, dans l'Aquifère du Néogène, en Belgique. Les eaux d'infiltration sont apparues faiblement minéralisées et de pH faible, du fait de la décalcification marquée des sédiments. Les augmentations

des concentrations en SiO₂ et cations en suivant les lignes de flux indiquent la présence de processus d'altération des silicates, confirmée à l'aide des indices de saturation, calculés avec PHREEQC, et des diagrammes d'équilibre. Un système de hiérarchisation basé sur les espèces redox sensibles a été développé, et montre qu'une chaîne d'oxydoréduction développée est présente dans l'aquifère. L'oxydation de la pyrite à faible profondeur entraîne une augmentation des sulfates, tandis que le fer précipite sous forme d'hydroxydes. Les concentrations élevées en arsenic sont liées à la réduction de ces hydroxydes de fer à faible profondeur, ainsi qu'à la dissolution de sidérite plus profondément. La dissolution des carbonates des formations aquifères, présents dans les couches profondes et au nord, entraîne une augmentation des concentrations en Ca²⁺ et HCO₃⁻. Le Ca²⁺ des eaux souterraines est échangé avec les ions Na⁺, Mg²⁺ et K⁺ adsorbés sur les feuillets d'argile au mur du réservoir. Même si l'Aquifère du Néogène est bien drainé, certaines influences marines rémanentes sont observables dans les secteurs les plus profonds.

Resumen Se estudió la evolución de la química de aguas subterráneas a lo largo del flujo de estas mediante el uso de datos hidroquímicos de muestras tomadas a lo largo de una línea de flujo en el acuífero Neogeno. Se encontró que el agua que se infiltra tiene un contenido mineral muy bajo y un pH bajo porque los sedimentos están altamente descalcificados. Un incremento en las concentraciones de SiO₂ y de cationes a lo largo de la línea de flujo de agua subterránea indica procesos de descomposición de silicatos, lo cual se confirma con el apoyo de índices de saturación calculados con PHREEQC y diagramas de estabilidad. Se desarrolló un sistema de clasificación basado en especies sensitivas redox. Este muestra que hay una secuencia de redox extensa en el acuífero. A poca profundidad la oxidación de pirita ha causado un incremento de sulfatos, mientras que el fierro se precipita como hidróxidos. Las concentraciones elevadas de arsénico se relacionan con la reducción de esos hidróxidos de fierro a nivel poco profundo y a la disolución de siderita a nivel más profundo. La disolución de carbonatos en el material del acuífero, presente a niveles profundos al norte ha llevado a un incremento de concentraciones de Ca²⁺ y HCO₃⁻. El Ca²⁺ de las agua subterráneas se intercambia por Na⁺, Mg²⁺ y K⁺ adsorbido en las

Received: 22 September 2004 / Accepted: 5 April 2006
Published online: 20 June 2006

© Springer-Verlag 2006

M. Coetsiers (✉) · K. Walraevens
Laboratory for Applied Geology and Hydrogeology,
Ghent University,
Krijgslaan 281-S8, B-9000, Ghent, Belgium
e-mail: Marleen.Coetsiers@UGent.be
Tel.: +32-9-2644657
Fax: +32-9-2644988

superficies de arcilla al fondo del reservorio de agua subterránea. A pesar de que el acuífero Neogeno tiene buena circulación algunas influencias marinas persisten en las partes más profundas.

Keywords Hydrochemistry · Groundwater flow · Redox reactions · Belgium

Introduction

The Neogene Aquifer lies in the northeast of Flanders, in the provinces of Antwerp and Limburg, Belgium, and is considered to be the most important groundwater reservoir in Flanders providing large amounts of drinking water. The sediments are mainly composed of sands deposited in shallow marine conditions with some continental facies. Groundwater extraction mostly takes place from deep wells in the Formations of Diest and Berchem to avoid near-surface effects such as high iron content or to avoid pollution by surface activities such as agriculture. Diffuse pollution from former metallurgic industries and mining activities is responsible for elevated Zn, Ni, Cd, Pb and Cu concentrations in the groundwater (Walraevens et al. 2003).

Natural geochemical processes play an important role in groundwater quality. The aim of this study is to characterize the natural chemical processes occurring in the Neogene Aquifer. In terms of space and depth, the chemistry of groundwater in the Neogene Aquifer is variable as a function of the geological and hydrogeological factors. Previous studies in the region did not deal with the evolution of groundwater quality along a flow line or on cross-sections but only looked at maps in a lateral context. The vertical variations in groundwater quality in the Neogene are very important in order to understand the natural evolution of the water quality. In order to determine the geochemical processes influencing groundwater quality in the Neogene Aquifer, the evolution of groundwater quality will be studied along a groundwater flow line.

Geological and hydrogeological setting

The Campine Basin in the northeast of Belgium is filled with sediments from the Miocene up to the Pleistocene age, which have marine and continental origins. These sediments dip gently towards the north–northeast with a slope of about 1–2% and are disturbed by different faults. The Boom Clay, a compact and silty clay (Vandenbergh 1978), forms the substratum of the groundwater body. A geological map of the area is given (Fig. 1) and Fig. 2 shows a schematic geological cross-section from NW to SE. The Miocene deposits have a marine origin and crop out in the south of the study area. They consist of fine to coarse glauconitic and micaceous sands. Locally, lignite, shells and iron sandstones can be present in these sands. Pliocene sediments were deposited under fluvial con-

ditions in the east with a gradual change to shallow marine environments towards the west. They consist of lignitic sands with clay lenses in the east and shelly sands in the west. During Pleistocene times, marine to estuarine sediments were deposited in the northwest of the study area. Pleistocene sediments are composed of sands with shells and clay lenses. In the northern part, the Pleistocene deposits contain an important clay layer in the middle, which has formed a cuesta in the landscape. A cuesta is an asymmetric landscape type, formed by the occurrence of a gently sloping succession of easily and hardly eroding sediment layers. The area in which the Pleistocene clay is present, is indicated on Fig. 1. During the development of the Roer Graben, which is the northwest branch of the Rhine Graben, faults were formed in the northern part of the province of Limburg (Limburg covers the eastern half of the area shown in Fig. 1; Camelbeeck and Meghraoui 1996; Demyttenaere and Laga 1988). Subsidence was very strong during the Mio- and Pliocene and is still active at present.

The Neogene Aquifer consists of the Mio- and Pliocene deposits up to the lower part of the Pleistocene deposits in the Campine Basin. Patyn et al. (1989) concluded from hydrogeological observations that, notwithstanding their lithologic differences, the Neogene sands behave as a single aquifer. From south to north, two different zones can be distinguished: in the south the Neogene Aquifer is unconfined, while, towards the north, the aquifer becomes semi-confined by the occurrence of clay lenses and layers in the Pleistocene deposits. Two main aquifers can thus be distinguished in the studied area: the Neogene Aquifer and the Pleistocene Aquifer, which are separated from each other by the Pleistocene Aquitard (Fig. 2). The Neogene Aquifer is well flushed and in most parts strongly decalcified. In the west and northwest of the study area (Fig. 1), the deposits contain up to 15% CaCO₃ (Van Dyck et al. 1981). The Miocene deposits are locally enriched in vivianite (De Meuter and Laga 1976).

The regional groundwater flow in the Neogene Aquifer was simulated by means of the three-dimensional modular model MODFLOW (Coetsiers et al. 2005; McDonald and Harbaugh 1988). The model consists of three layers: the Pleistocene Aquifer, the Pleistocene Aquitard and the Neogene Aquifer. The calculated piezometric heads under natural conditions in the Neogene Aquifer are presented in Fig. 3. Groundwater recharge takes place mainly in the topographically elevated areas like the Campine Plateau in the southeast and the cuesta of the Pleistocene Aquitard in the northwest. Smaller recharge areas are present in hilly areas in the south, where remnant hills form a topographical elevation. Natural groundwater flow is mainly radial from the Campine Plateau. Groundwater infiltrating on the eastern and northern flanks flows into the Meuse River Basin, whereas groundwater recharged on the western side joins the Scheldt River Basin. The Pleistocene Clay cuesta gives rise to a groundwater divide in the north of the studied area. Water infiltrating on the northern cuesta backslope flows towards the Meuse River Basin in the

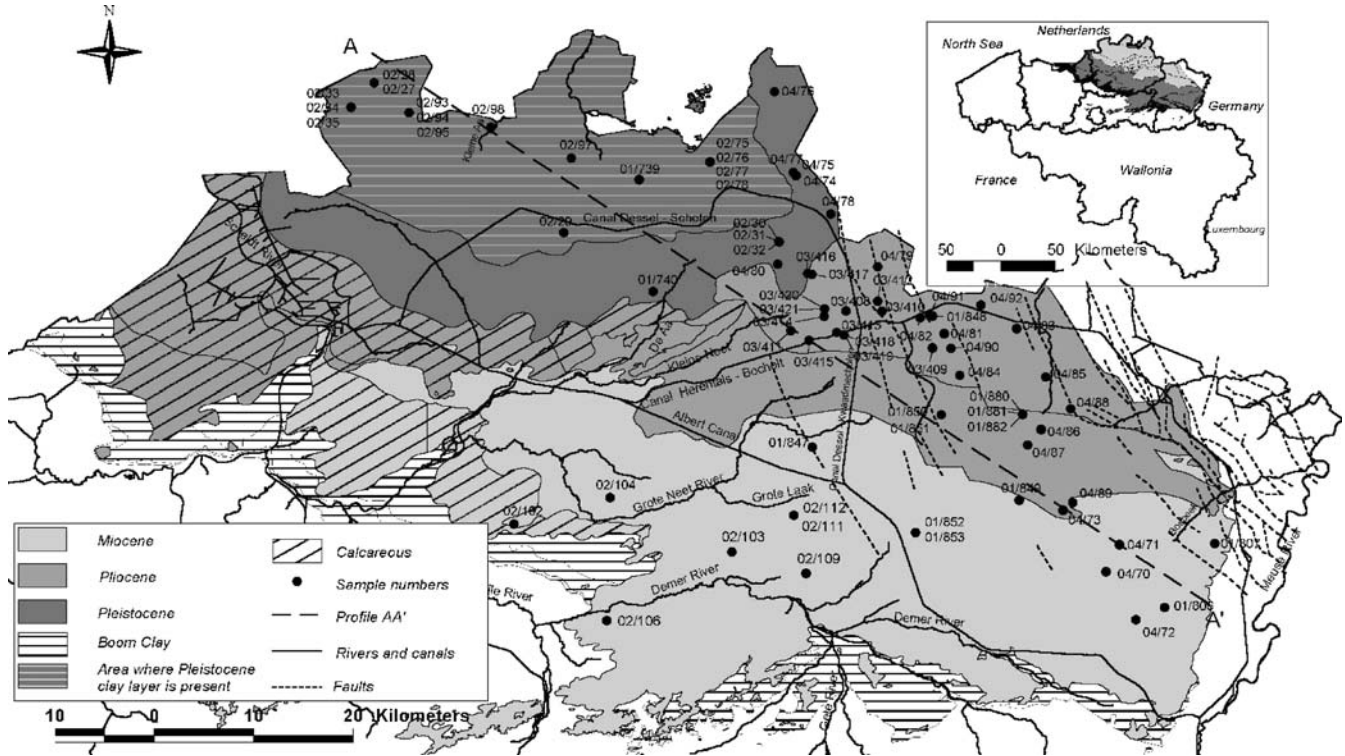


Fig. 1 Location and geological map of the Neogene Aquifer with indication of groundwater sample numbers

Netherlands, while water recharging on the southern cuesta scarp flows towards the Scheldt River Basin. Groundwater discharge takes place by means of rivers

and rivulets in the saddle-shaped valley between the Pleistocene clay cuesta in the north and the hilly areas in the south and on the cuesta backslope in the north.

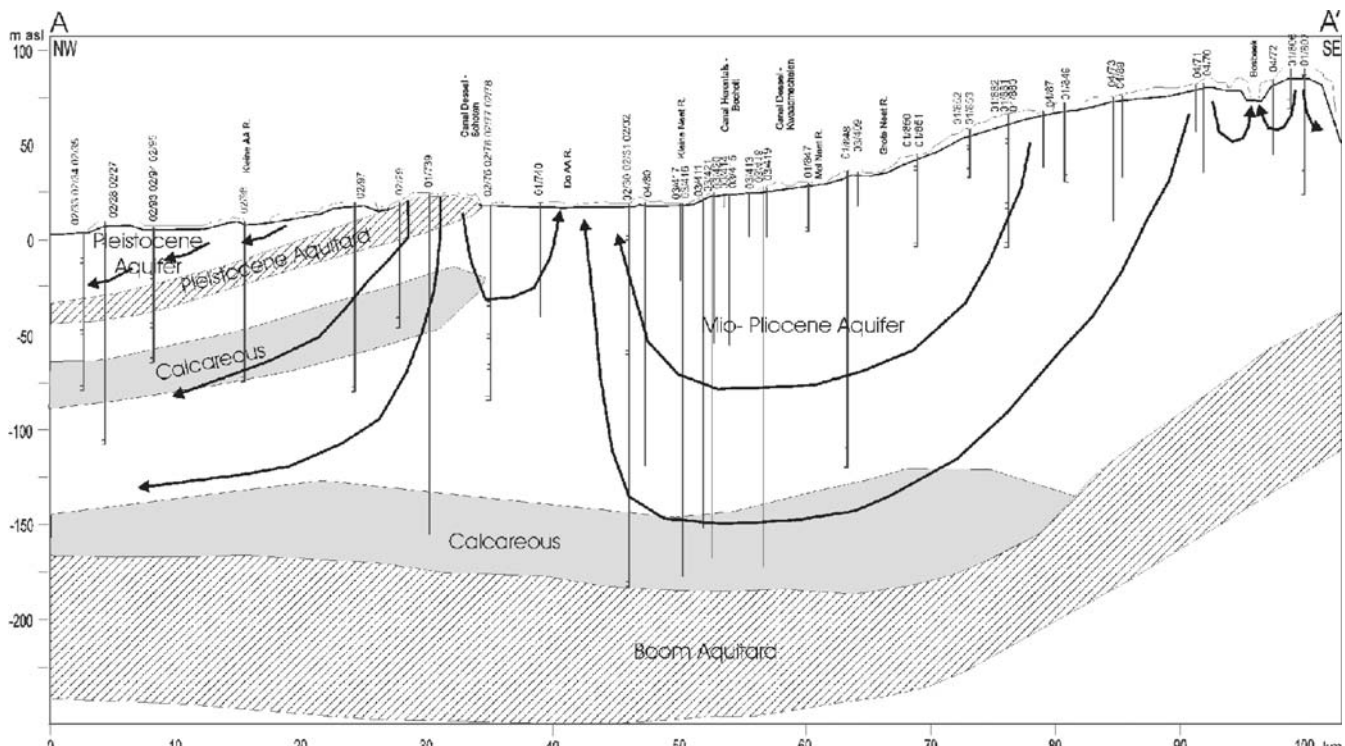


Fig. 2 Hydrogeological cross-section of the Neogene Aquifer with indication of the position of the sampled well screens and groundwater flow direction (the location of the profile AA' is indicated on Fig. 1)

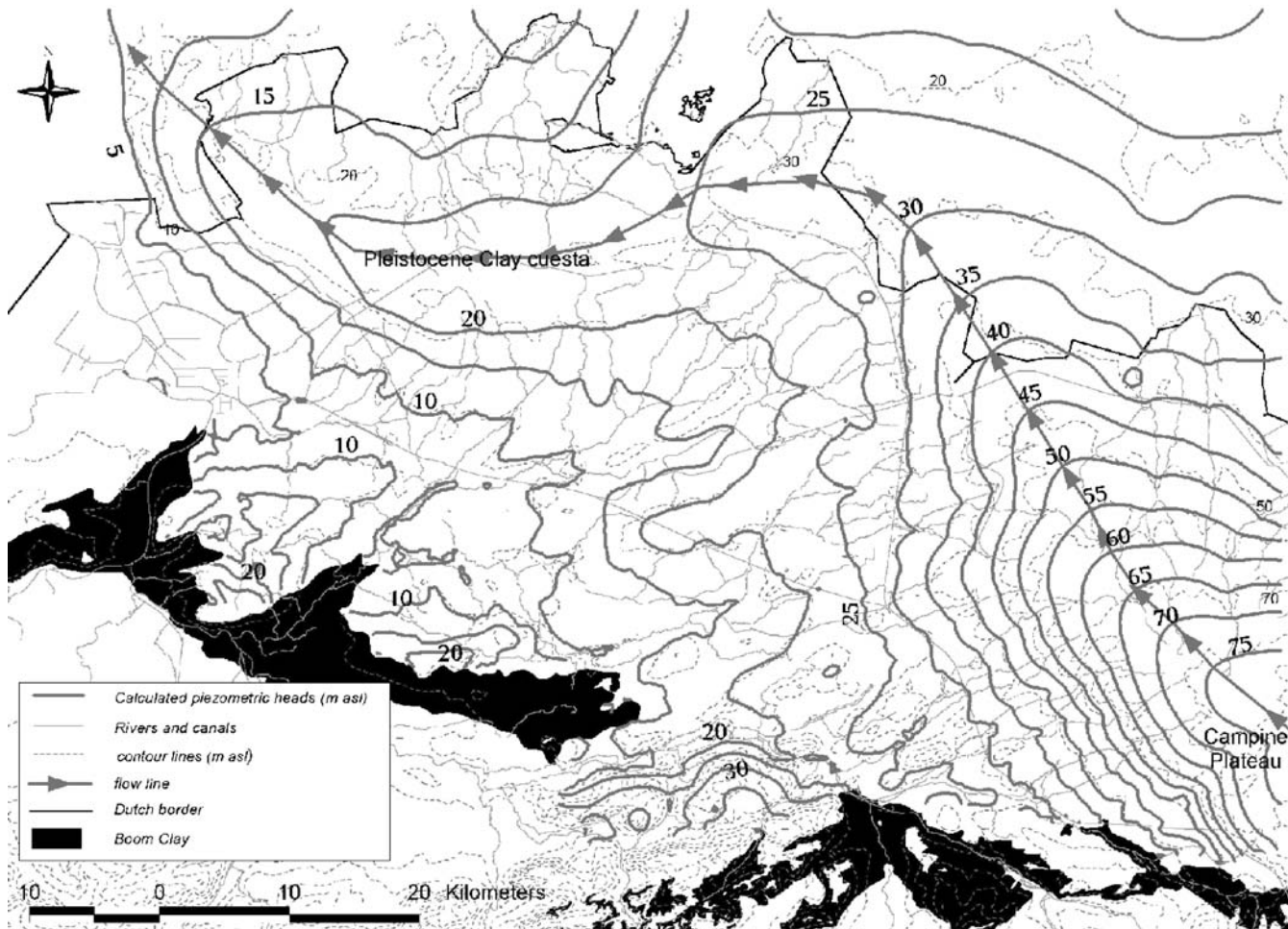


Fig. 3 Contour map of piezometric heads in the mio- pliocene aquifer calculated with visual MODFLOW (Coetsiers et al. 2005)

Sampling and analytical methods

Seventy-seven groundwater samples from 60 wells in the Neogene Aquifer were collected during field campaigns carried out between 2001 and 2004. Some wells had several screens at different depths (Table 1). All screens were sampled once. The parameters pH, dissolved oxygen (DO) and redox potential (Eh) were measured on-site in an anaerobic flow-through cell. Other on-site measurements included temperature and electrical conductivity (EC). Where an oxygen-free measurement was not possible (samples taken from the tap at industrial companies), these parameters were measured immediately after sampling in the field. Furthermore, the alkalinity was measured in the field, since disturbance in the carbonate equilibrium can occur by CO₂ contact or escape from the sample.

The samples were analysed at the Laboratory for Applied Geology and Hydrogeology (LTGH), Ghent University. Samples for laboratory analysis were filtered through 0.45-μm membranes in order to remove colloidal or suspended particles. The samples were taken in glass or polyethylene flasks and if necessary acidified or fixated in accordance with standard methods for preservation of groundwater samples. Determination of cations was done

by means of Flame Atomic Absorption Spectrophotometry (FAAS). Also arsenic was measured by FAAS following hydride generation. Other trace elements were analysed by means of graphite furnace atomic absorption spectrophotometry (GFAAS). Most of the anions were measured with molecular absorption spectrophotometry, while chloride was measured with a chloridometer and fluoride with an ion-selective electrode. For all samples, the error on the ionic balance was smaller than 5% and in most cases smaller than 2%. Table 1 shows the screen depth, date of sampling, pH, and EC for the 77 samples. The locations of the groundwater sampling points are indicated in Fig. 1.

Results and discussion

The classification system of Stuyfzand (1986), which takes cation exchange into account, was applied to the chemical data (Table 1; Fig. 4). All groundwater in the Neogene Aquifer is fresh (code F, Cl<150 mg L⁻¹) and very soft to hard (code *, 0, 1 and 2). Shallow groundwater is very soft and is mostly of the CaSO₄, FeSO₄, MgSO₄, CaMix, FeMix, NaMix or CaCl water

Table 1 Analytical data and Stuyfzand classification (Stuyfzand 1986) for groundwater samples of the neogene aquifer

| Sample | Screen depth (m) | Date | pH | EC µS/cm 25°C | Water type (Stuyfzand 1986) | Sample | Screen depth (m) | Date | pH | EC µS/cm 25°C | Water type (Stuyfzand 1986) |
|--------|---------------------|------------|-----|------------------|--|--------|---------------------|------------|-----|------------------|---|
| 01/739 | 180.00 | 07/12/2001 | 7.2 | 489 | F1-NaHCO ₃ + F2-CaHCO ₃₀ F*-CaHCO ₃ 0 | 02/111 | 10.00 | 24/01/2002 | 5.5 | 109 | F*-FeMix 0 F*-CaSO ₄ 0 F*-NaHCO ₃ + |
| 01/740 | 68.00 | 07/12/2001 | 7.3 | 329 | | 03/409 | 18.00 | 25/03/2003 | 6.0 | 110 | |
| 01/807 | 64.38 | 13/12/2001 | 5.6 | 12 | | 03/408 | 204.00 | 25/03/2003 | 8.1 | 255 | |
| 01/806 | 20.13 | 13/12/2001 | 4.5 | 72 | F*-CaMmix 0 | 03/411 | 176.00 | 25/03/2003 | 8.2 | 285 | F*-NaHCO ₃ + F1-CaHCO ₃ + |
| 01/848 | 157.00 | 17/12/2001 | 6.9 | 62 | F*-CaHCO ₃ 0 | 03/410 | 314.00 | 25/03/2003 | 7.9 | 177 | F1-CaMmix + F1-CaMix + |
| 01/849 | 42.12 | 17/12/2001 | 6.1 | 61 | F*-CaHCO ₃ 0 | 03/412 | 45.00 | 25/03/2003 | 6.5 | 556 | F*-CaMmix 0 F*-KHC03 + |
| 01/847 | 25.52 | 17/12/2001 | 5.9 | 62 | F0-CaMmix 0 | 03/417 | 40.00 | 26/03/2003 | 6.4 | 124 | |
| 01/851 | 48.98 | 18/12/2001 | 4.8 | 66 | F*-CaHCO ₃ + F*-CaSO ₄ 0 | 03/415 | 82.00 | 26/03/2003 | 8.0 | 266 | |
| 01/850 | 8.98 | 18/12/2001 | 6.1 | 161 | | 03/416 | 196.00 | 26/03/2003 | 8.6 | 343 | F*-NaHCO ₃ + F0-CaSO ₄ + |
| 01/852 | 10.49 | 18/12/2001 | 5.6 | 117 | F*-FeHCO ₃ 0 | 03/414 | 7.00 | 26/03/2003 | 6.4 | 320 | F0-NaHCO ₃ + F0-NaHCO ₃ + |
| 01/853 | 25.49 | 18/12/2001 | 5.9 | 127 | F0-CaMmix + | 03/413 | 25.00 | 26/03/2003 | 9.4 | 250 | |
| 01/882 | 70.00 | 20/12/2001 | 6.0 | 114 | F*-FeSO ₄ 0 | 03/419 | 27.00 | 27/03/2003 | 5.1 | 285 | F*-NaSO ₄ 0 F0-CaHCO ₃ + |
| 01/881 | 50.00 | 20/12/2001 | 5.4 | 145 | F0-CaSO ₄ + | 03/420 | 80.00 | 27/03/2003 | 7.3 | 129 | F0-MgHCO ₃ + F0-CaCl 0 |
| 01/880 | 15.00 | 20/12/2001 | 5.9 | 332 | F1-CaSO ₄ + | 03/418 | 200.00 | 27/03/2003 | 8.7 | 220 | F1-CaHCO ₃ 0 F0-NaHCO ₃ + |
| 02/229 | 66.00 | 03/01/2002 | 6.8 | 95 | F1-CaHCO ₃ + F2-CaHCO ₃ + | 03/421 | 193.00 | 27/03/2003 | 8.8 | 243 | |
| 02/227 | 117.50 | 03/01/2002 | 5.2 | 228 | | 04/72 | 40.00 | 24/02/2004 | 6.1 | 91 | |
| 02/228 | 11.50 | 03/01/2002 | 4.8 | 340 | F2-CaSO ₄ + | 04/72 | 25.00 | 24/02/2004 | 7.1 | 211 | F0-CaMmix 0 F0-CaHCO ₃ + |
| 02/322 | 209.74 | 04/01/2002 | 6.6 | 130 | F0-CaHCO ₃ + | 04/70 | 50.00 | 24/02/2004 | 5.2 | 233 | F*-CaSO ₄ 0 F*-CaHCO ₃ 0 |
| 02/30 | 19.85 | 04/01/2002 | 5.6 | 77 | F0-CaMmix 0 | 04/73 | 61.00 | 25/02/2004 | 6.6 | 136 | F1-CaHCO ₃ + F1-CaSO ₄ 0 |
| 02/31 | 81.76 | 04/01/2002 | 6.5 | 87 | F2-CaHCO ₃ + | 04/74 | 232.00 | 25/02/2004 | 7.9 | 464 | |
| 02/35 | 82.84 | 07/01/2002 | 6.7 | 104 | F1-CaHCO ₃ + | 04/75 | 70.00 | 25/02/2004 | 5.7 | 412 | |
| 02/34 | 53.87 | 07/01/2002 | 5.1 | 155 | F1-CaSO ₄ + | 04/78 | 248.00 | 01/03/2004 | 8.2 | 270 | F*-NaHCO ₃ + F0-MgHCO ₃ + |
| 02/33 | 15.9 | 07/01/2002 | 4.8 | 130 | F1-MgSO ₄ + | 04/79 | 272.00 | 01/03/2004 | 8.1 | 193 | F0-CaHCO ₃ + F0-NaHCO ₃ + |
| 02/75 | 52.84 | 09/01/2002 | 5.8 | 117 | F0-CaMmix 0 | 04/76 | 222.00 | 01/03/2004 | 7.8 | 422 | F2-CaHCO ₃ + F0-MgHCO ₃ + |
| 02/76 | 69.81 | 09/01/2002 | 6.7 | 122 | F1-CaHCO ₃ + | 04/77 | 212.00 | 01/03/2004 | 7.8 | 462 | |
| 02/77 | 86.81 | 09/01/2002 | 6.9 | 125 | F1-CaHCO ₃ + | 04/82 | 170.00 | 02/03/2004 | 7.1 | 120 | F0-CaHCO ₃ + F*-NaHCO ₃ + |
| 02/78 | 102.81 | 09/01/2002 | 7.0 | 11 | F2-CaHCO ₃ + | 04/80 | 140.00 | 02/03/2004 | 8.4 | 407 | F0-CaHCO ₃ + F0-CaHCO ₃ + |
| 02/94 | 53.84 | 10/01/2002 | 5.4 | 67 | F*-CaHCO ₃ 0 | 04/83 | 192.00 | 02/03/2004 | 7.9 | 156 | |
| 02/93 | 26.86 | 10/01/2002 | 5.3 | 94 | F*-CaMmix 0 | 04/84 | 175.00 | 02/03/2004 | 7.8 | 422 | F0-CaHCO ₃ + F0-CaHCO ₃ + |
| 02/95 | 70.82 | 10/01/2002 | 6.6 | 130 | F2-CaHCO ₃ + | 04/81 | 300.00 | 02/03/2004 | 8.1 | 214 | F0-MgHCO ₃ + F0-CaHCO ₃ + |
| 02/97 | 100.00 | 15/01/2002 | 6.9 | 132 | F1-CaHCO ₃ + | 04/85 | 247.00 | 03/03/2004 | 7.3 | 182 | F0-CaHCO ₃ + F0-CaHCO ₃ + |
| 02/98 | 84.50 | 15/01/2002 | 6.9 | 447 | F2-CaHCO ₃ + | 04/88 | 50.00 | 03/03/2004 | 7.8 | 286 | |
| 02/103 | 24.80 | 21/01/2002 | 6.0 | 631 | F2-CaMmix + | 04/86 | 50.00 | 03/03/2004 | 6.1 | 336 | F0-CaSO ₄ 0 F0-CaHCO ₃ + |
| 02/104 | 24.87 | 22/01/2002 | 5.7 | 132.2 | F0-CaHCO ₃ + | 04/87 | 30.00 | 03/03/2004 | 5.8 | 334 | |
| 02/102 | 24.80 | 22/01/2002 | 7.1 | 282 | F1-CaHCO ₃ + | 04/89 | 43.00 | 04/03/2004 | 6.4 | 121 | F*-FeMix 0 F0-CaHCO ₃ + |
| 02/109 | 58.00 | 23/01/2002 | 5.8 | 84 | F*-CaHCO ₃ 0 | 04/91 | 300.00 | 04/03/2004 | 8.1 | 180 | F0-CaHCO ₃ + F0-CaHCO ₃ 0 |
| 02/106 | 9.20 | 23/01/2002 | 6.7 | 150 | F1-CaHCO ₃ + | 04/90 | 153.00 | 04/03/2004 | 7.0 | 171 | |
| 02/107 | 34.87 | 23/01/2002 | 6.8 | 133 | F1-CaHCO ₃ + | 04/92 | 304.00 | 04/03/2004 | 7.9 | 237 | |
| 02/112 | 20.00 | 24/01/2002 | 5.4 | 120 | F*-FeMix + | | | | | | |

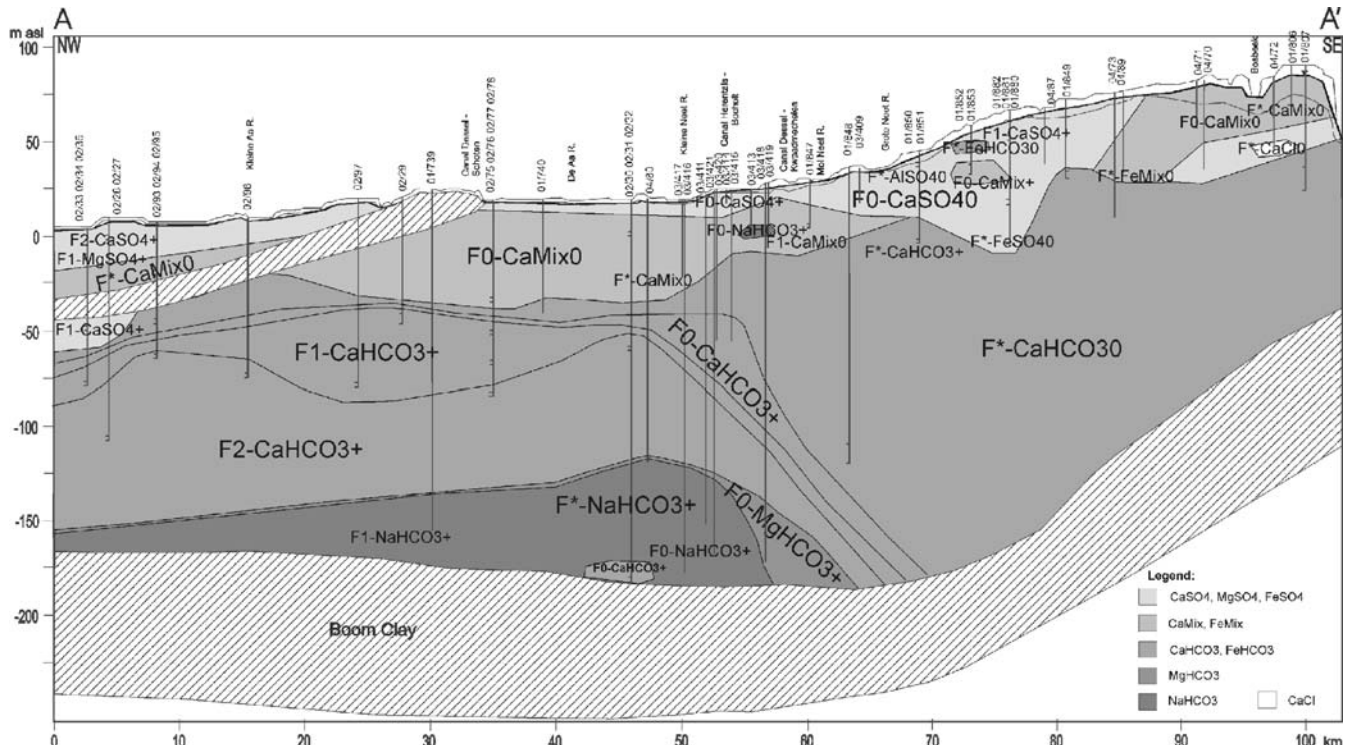


Fig. 4 Stuyfzand (1986) classification presented in profile AA'. Code F denotes fresh groundwater that ranges from 'very soft' to 'hard' (progressively denoted by *, 0, 1 and 2)

type. Infiltrating groundwater has a NaCl water type as it is derived from meteoric water. Since calcite is not present here in the unsaturated zone, calcite dissolution cannot influence the water quality. Pyrite oxidation in the unsaturated zone is responsible for the occurrence of CaSO_4 and FeSO_4 groundwater types. Furthermore, agricultural pollution gives rise to the local appearance of CaNO_3 water types in shallow wells. Reactions such as the oxidation of organic matter increase the HCO_3^- content, leading to the occurrence of CaMix water types. Deeper in the aquifer, groundwater becomes CaHCO_3 water type and is still very soft to soft. The cation exchange code is added at the end of the classification name by a positive, neutral or negative sign. A positive cation exchange code indicates groundwater with a (Na+K+Mg)-surplus and is mostly related to freshening conditions. However, elevated Na, K or Mg concentrations can also be caused by pollution from fertilizers or weathering of silicates and can cause a positive cation exchange code (Stuyfzand 1986). In the deeper parts of the aquifer, the cation exchange parameter becomes positive indicating groundwater with a (Na+K+Mg)-surplus. In the deepest parts of the aquifer, MgHCO_3 and NaHCO_3 groundwater types occur indicating the existence of cation exchange resulting from freshening (Walraevens and Van Camp 2005). In Fig. 5, the evolution of water types can be observed in a Piper diagram. In the lower part of the Piper diagram, the evolution from CaHCO_3 to MgHCO_3 and NaHCO_3 indicate cation exchange as the major freshening process.

The evolution of different groundwater quality parameters along a groundwater flow line, indicated on Fig. 3, is

presented in Fig. 6. Groundwater in the Neogene Aquifer has a very low mineral content. Total dissolved solids (TDS) increases from 44 to 620 mg L^{-1} in the direction of flow. Electrical conductivity (EC) ranges from 11 to $489 \mu\text{S cm}^{-1}$ (at 25°C) and pH ranges from 4.5 to 8.3 (Fig. 6; Table 1). Thus, TDS, EC and pH all increase along the direction of groundwater flow. Bicarbonate concentration in the Neogene Aquifer system is very low to moderately high and varies between 2 and 440 mg L^{-1} . The bicarbonate concentrations are very low in the shallow samples and increase along the groundwater flow line (Fig. 6). In the shallow part, the aquifer is decalcified so that calcite dissolution cannot occur. Only to the north and in the deeper parts, carbonate rich layers are present (grey zones in Fig. 2) and calcite dissolution can affect groundwater quality, leading to high bicarbonate and calcium concentrations and high pH (Fig. 6). The saturation index with respect to calcite was calculated by means of the programme PHREEQC2 (Parkhurst and Appelo 1999) and is represented in Fig. 7 along the flow line. Most groundwaters in the region are undersaturated with respect to calcite. The strongest subsaturation occurs in the shallow decalcified part of the aquifer, whereas in the carbonate-rich layers, the saturation index indicates that close to saturation and even slightly supersaturated samples have been found.

Along the groundwater flow line, a strong increase in phosphate concentration can be observed with a maximum between 30 and 40 km and from 70 to 120 km (Fig. 6). The saturation index for vivianite calculated with PHREEQC indicates close to saturation between 15 and

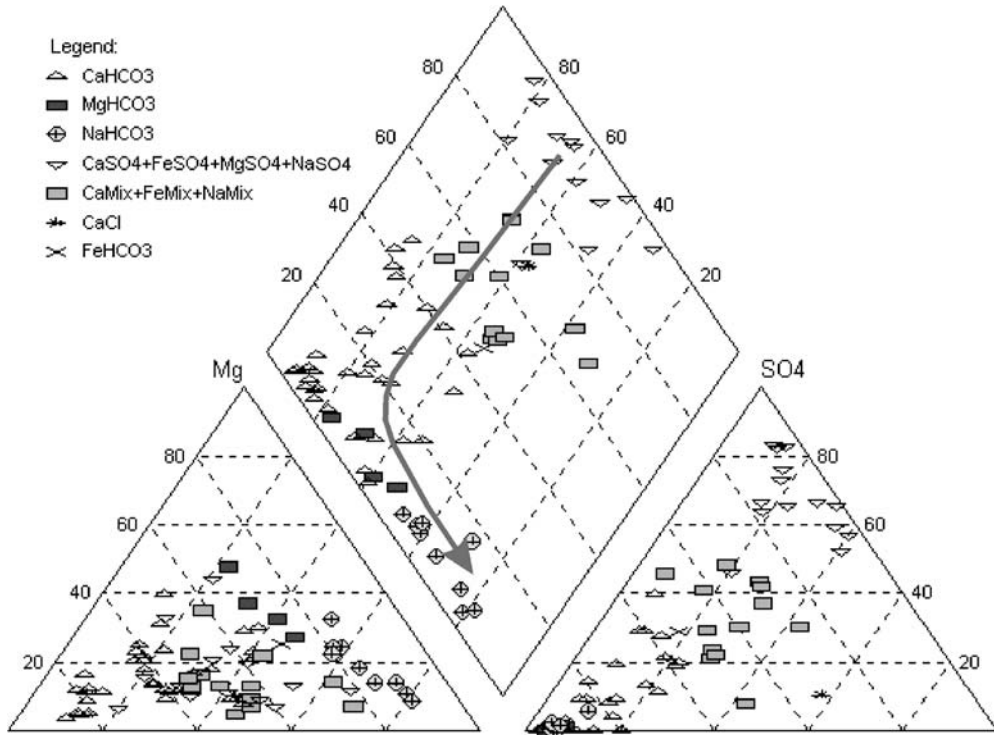


Fig. 5 Piper diagram with indication of groundwater type (major ions) from 77 samples. The arrow represents the evolution of groundwater along a groundwater flow line

40 km and between 70 and 120 km, while in the other parts of the groundwater reservoir, strong subsaturation is observed (Fig. 7). The dissolution of vivianite ($\text{Fe}_3(\text{PO}_4)_2 \cdot 8\text{H}_2\text{O}$), locally present in the sediments, is responsible for this increase in phosphate concentrations. After 40 km, the phosphate concentrations decrease again. The saturation index for vivianite also decreases after 40 km. This decrease in the saturation index can be explained by the simultaneous removal of iron from the groundwater (Fig. 6) caused by the formation of iron sulphides in the sulphate-reducing zone. In Fig. 7, the saturation index for hydroxyapatite [$\text{Ca}_{10}(\text{PO}_4)_6(\text{OH})_2$] is also represented. It can be seen that groundwater from the first 30 km is strongly subsaturated with respect to hydroxyapatite, while groundwater further along the flow line is close to saturation and in some cases oversaturated compared to hydroxyapatite. Phosphate will, in those waters, be removed by the precipitation of hydroxyapatite. The zone in between 30 and 40 km is probably rich in vivianite, resulting in high concentrations of phosphate.

The SiO_2 , Na, K, Mg and Ca-concentrations increase along the direction of groundwater flow (Fig. 6). Although it proceeds very slowly, silicate weathering can add silica and cations (Na^+ , K^+ , Mg^{2+} and Ca^{2+}) to the groundwater. As a result of this weathering, secondary minerals like clays (illite, kaolinite and montmorillonite) and iron oxides are usually formed during silicate weathering due to the insolubility of the Al-compounds (Appelo and Postma 1993). Saturation indices for albite (Na-plagioclase) and anorthite (Ca-plagioclase), used as end members of the

plagioclases, were calculated with PHREEQC2 (Parkhurst and Appelo 1999). Groundwater in the Neogene Aquifer is undersaturated with respect to albite and anorthite. The shallow samples are subsaturated with respect to K-feldspars while samples further along a flow line are oversaturated. Most groundwaters have a positive saturation index for kaolinite. From an equilibrium point of view, dissolution of plagioclases is thus possible. However, the problem with this approach is that Al^{3+} is often below detection limit or is in colloidal form, meaning that the saturation index cannot be calculated. Therefore, relations among solutions and aluminosilicate minerals are often depicted on an activity diagram. In Fig. 8, 63 groundwater samples are plotted on activity diagrams for the Ca-, Na- and K-feldspar systems. For the remaining 14 samples, silicium was not determined. On the anorthite and albite stability diagrams, all samples plot in the kaolinite field, thus, compared to the considered phases, kaolinite is here stable. These groundwaters are not in equilibrium with anorthite and albite, which will decompose if available in the reservoir. On the K-feldspar diagram, most of the samples also fall in the kaolinite stability field. The deep groundwater samples, however, plot in the muscovite stability field or at the top of the kaolinite stability field. This means that in shallow groundwater K-feldspar will decompose, while in deeper groundwater the saturation index prevents this process from going on. On the stability diagrams, the solubility of quartz and amorphous SiO_2 is also indicated. All groundwaters are supersaturated compared to quartz and subsaturated compared to amorphous SiO_2 . From the stability diagrams and the saturation

indices, it can be concluded that the weathering of Na-, K- and Ca-feldspars is theoretically possible.

The sulphate and iron content in groundwater drops very sharply at a distance of about 40 km along the flow line (Fig. 6). These changes in groundwater quality can be

explained by the occurrence of redox reactions. In a closed groundwater system, oxidation of organic matter is observed first by the reduction of O_2 followed by the reduction of NO_3^- , MnO_2 and Fe-oxides and hydroxides. When the environment is sufficiently reducing, fermenta-

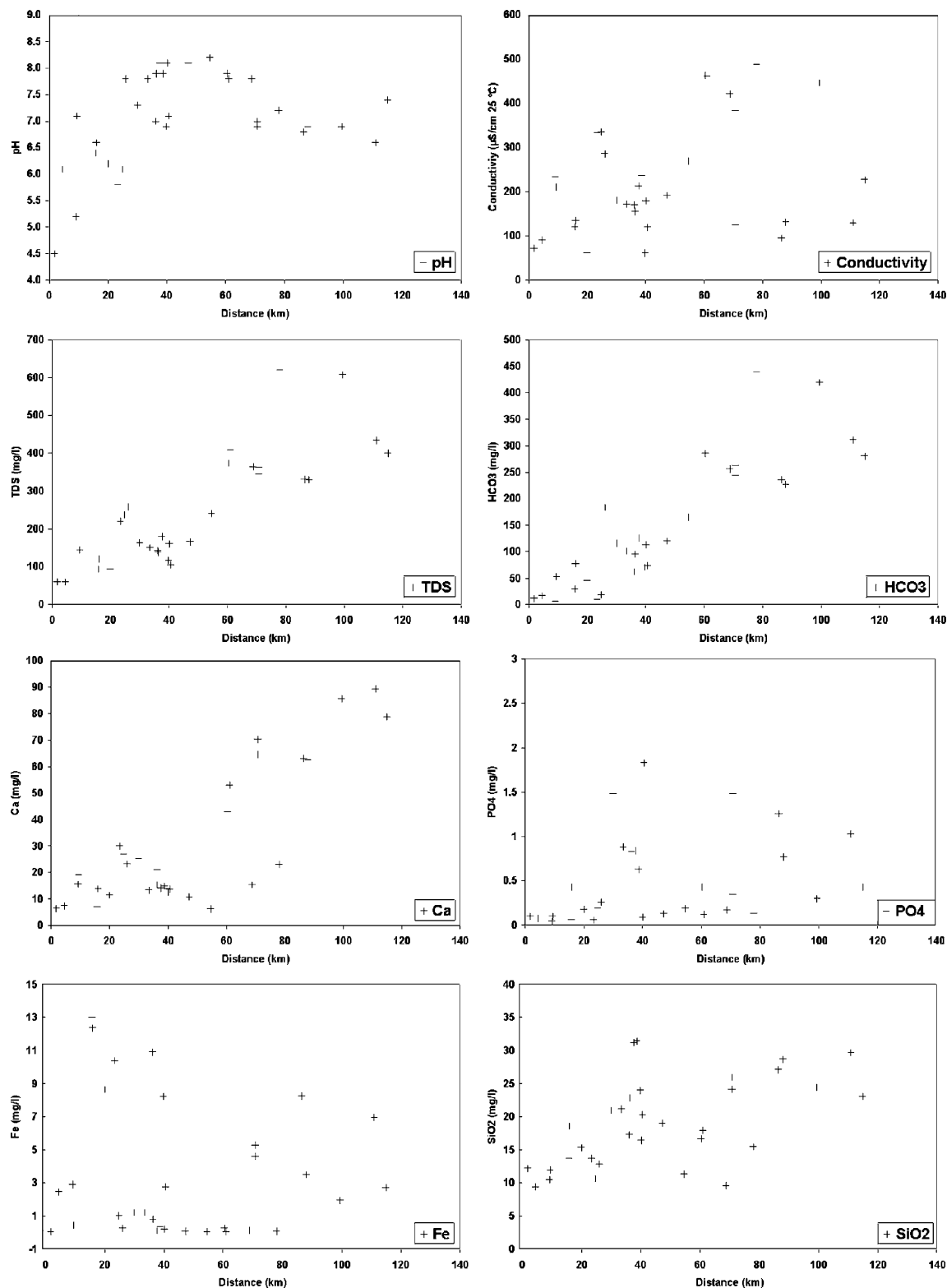
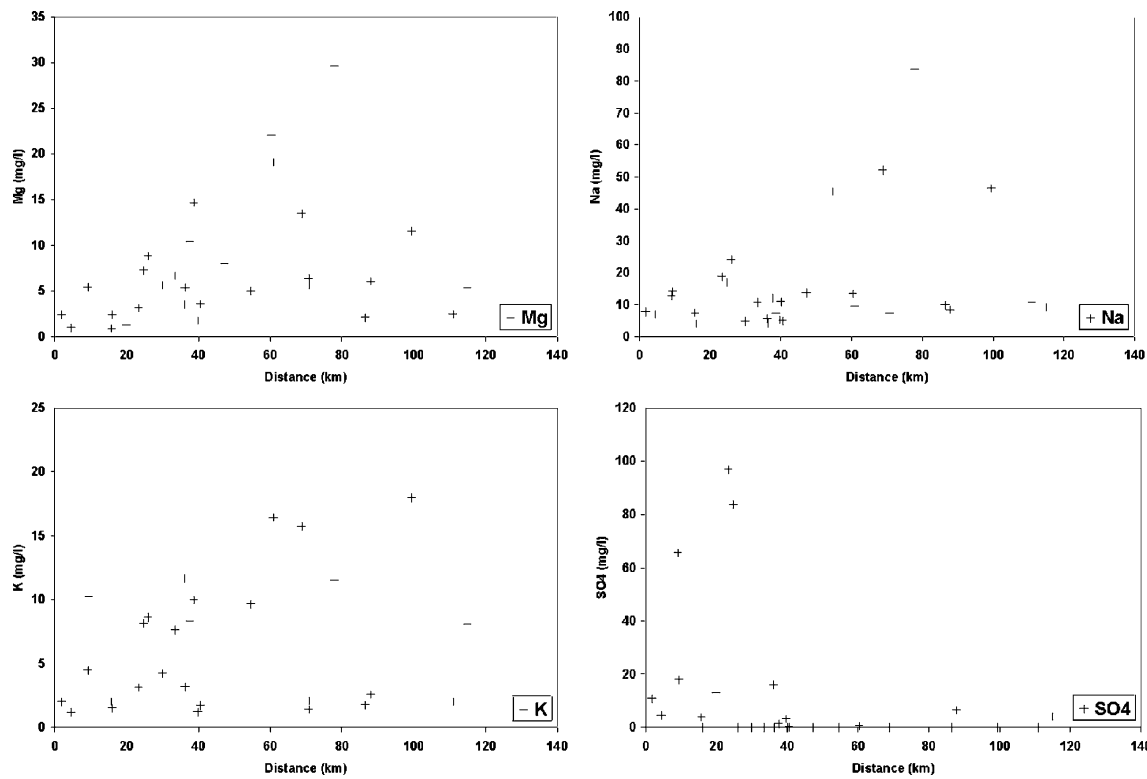


Fig. 6 Chemical parameters plotted along flow line (indicated on Fig. 3), with distance (km) measured from the Campine Plateau

Fig. 6 (continued)



tion reactions and reduction of SO_4^{2-} and CO_2 may occur at almost the same redox-potential (Stumm and Morgan 1981). The succession of these different redox zones can be recognized in the Neogene Aquifer. Hunter et al. (1998) underline that it is impossible to define the redox conditions by means of a unique Eh or pe value. Nevertheless, the redox level can be deduced empirically from the redox sensitive dissolved substances like O_2 , NO_3^- , Mn^{2+} , $\text{Fe}^{2+/3+}$, SO_4^{2-} , and CH_4 (Stumm 1984; Berner 1981). Stuyfzand (1993) and Pannatier et al. (2000) state that nitrate and sulphate can be considered to be good indicators to deduce the prevailing redox conditions. Dissolved oxygen and methane are often not measured and the measured values are frequently of a questionable quality.

A tree diagram for the determination of the redox level was constructed, adapted from the one shown by Pannatier et al. (2000), and is shown in Fig. 9. In brackish and salt water, the sulphate content is raised by the marine component. For this reason, groundwater samples are divided into two groups based on the Cl^- concentration. Fresh groundwater ($\text{Cl}^- < 150 \text{ mg L}^{-1}$) with sulphate concentrations lower than 5 mg L^{-1} is classified as 'sulphate reduced'. If the methane concentration is higher than 1 mg L^{-1} , groundwater is classified as 'methanogenic'. When the sulphate concentration is higher than 5 mg L^{-1} , sulphate reduction is considered to be still in process. The next parameter that conveys important information about the redox condition of the groundwater

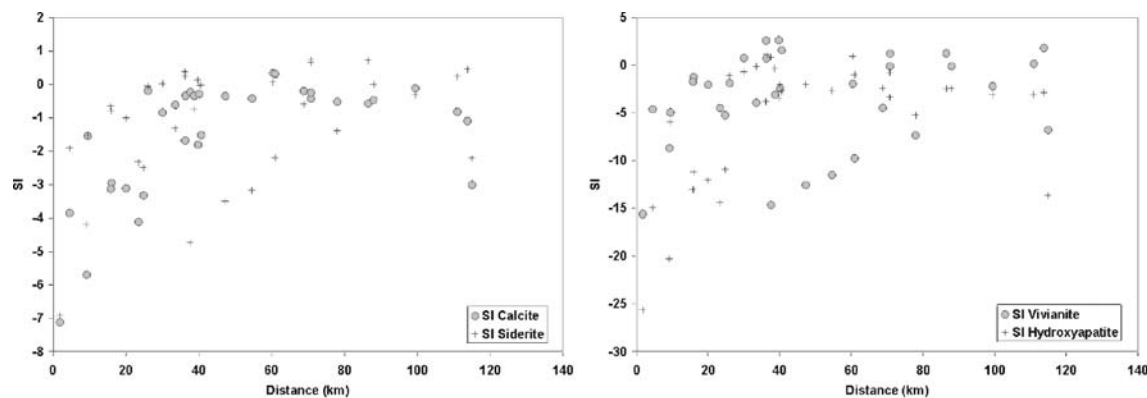


Fig. 7 Saturation index (SI) for calcite, vivianite, and hydroxyapatite along the flow line calculated with PHREEQC2

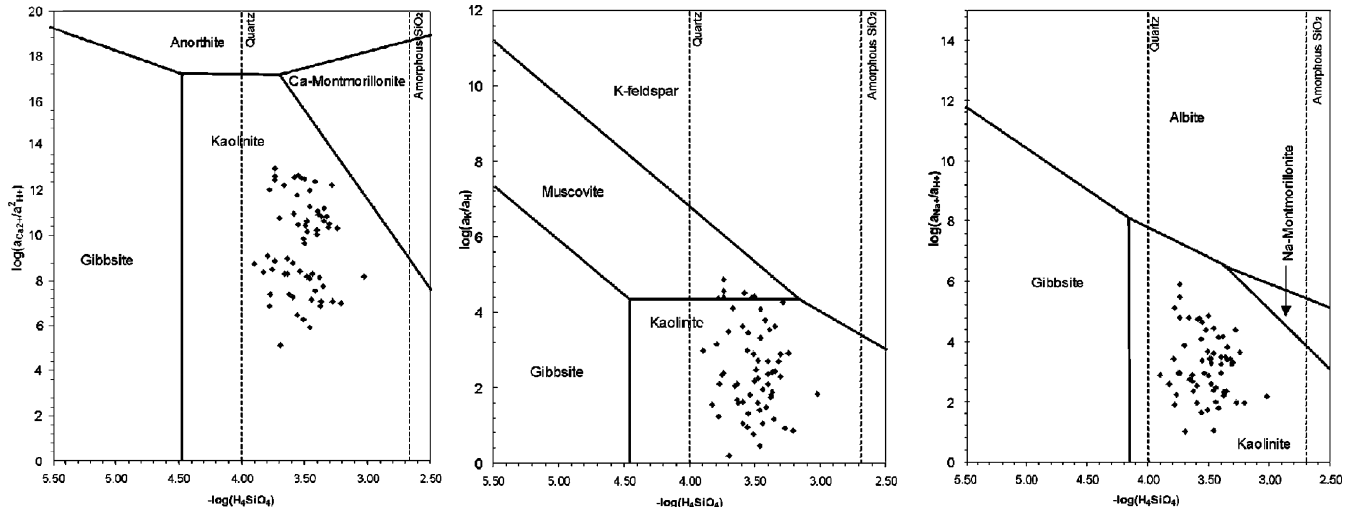


Fig. 8 Groundwater samples plotted on stability diagrams (at 25°C) for the Ca-, Na-, and K-feldspar systems and their possible weathering products. A groundwater sample that plots in the kaolinite field indicates kaolinite is more likely to be a stable mineral for this water composition than for example gibbsite

is iron: high iron concentrations occur after nitrate and manganese-oxides have been reduced. When the sample has an iron concentration larger than 1 mg L⁻¹, it is classified as ‘Fe-oxides reduced’. When the iron concentration is lower than 1 mg L⁻¹, the manganese content is evaluated. If Mn²⁺>0.5 mg L⁻¹, Mn-oxides have been reduced and the sample is classified as ‘Mn-oxides reduced’. When Mn²⁺<0.5 mg L⁻¹, nitrate will be the next evaluated parameter. Groundwater with a nitrate concentration less than 2 mg L⁻¹ comes from the nitrate reduced zone. A nitrate concentration larger than

2 mg L⁻¹ indicates nitrate reduction has not terminated yet and dissolved oxygen will be evaluated. If O₂>2 mg L⁻¹, the groundwater is called ‘oxic’ and, in the other case, groundwater is called ‘suboxic’. Because measurements of O₂ and CH₄ are often not available or the accuracy of the data is doubtful, it is often difficult to distinguish between the oxic and suboxic zones on one hand, and between the sulphate-reduced and methanogenic zones on the other. For this reason, these zones are often referred to as “oxic/suboxic” and “sulphate reduced/methanogenic”.

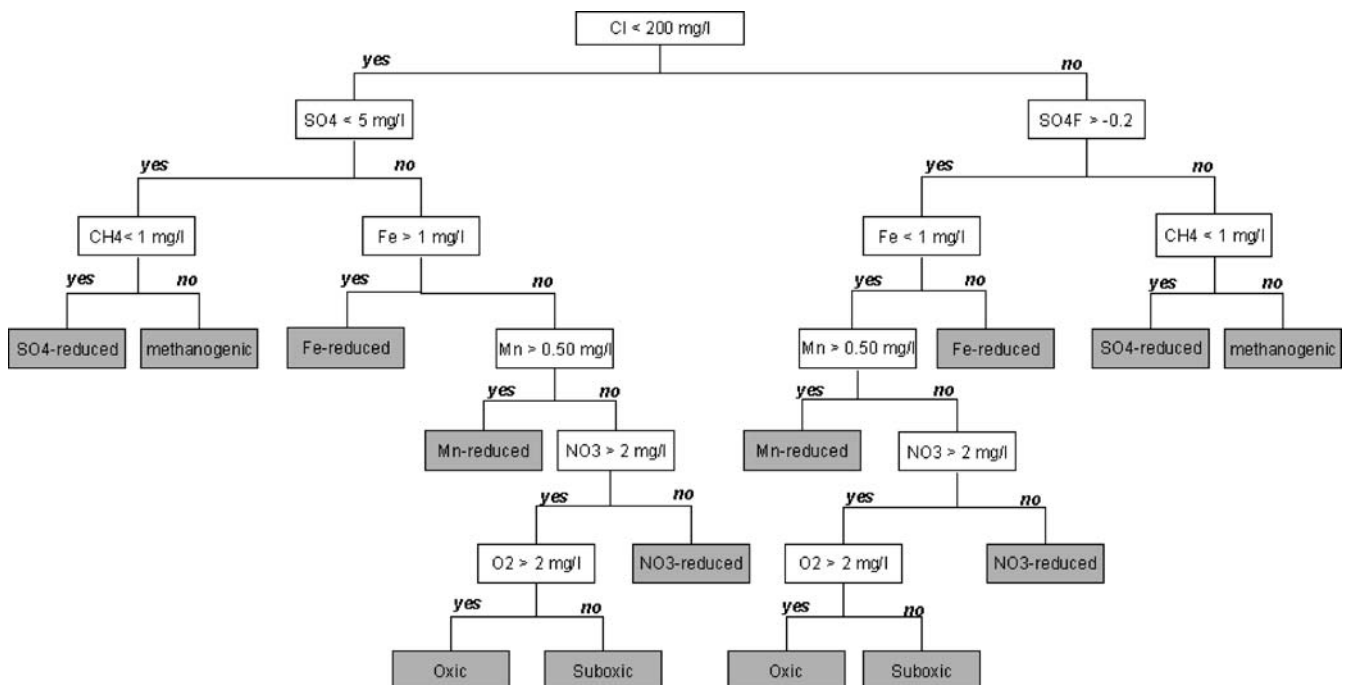


Fig. 9 Tree diagram for deducing the redox level in groundwater

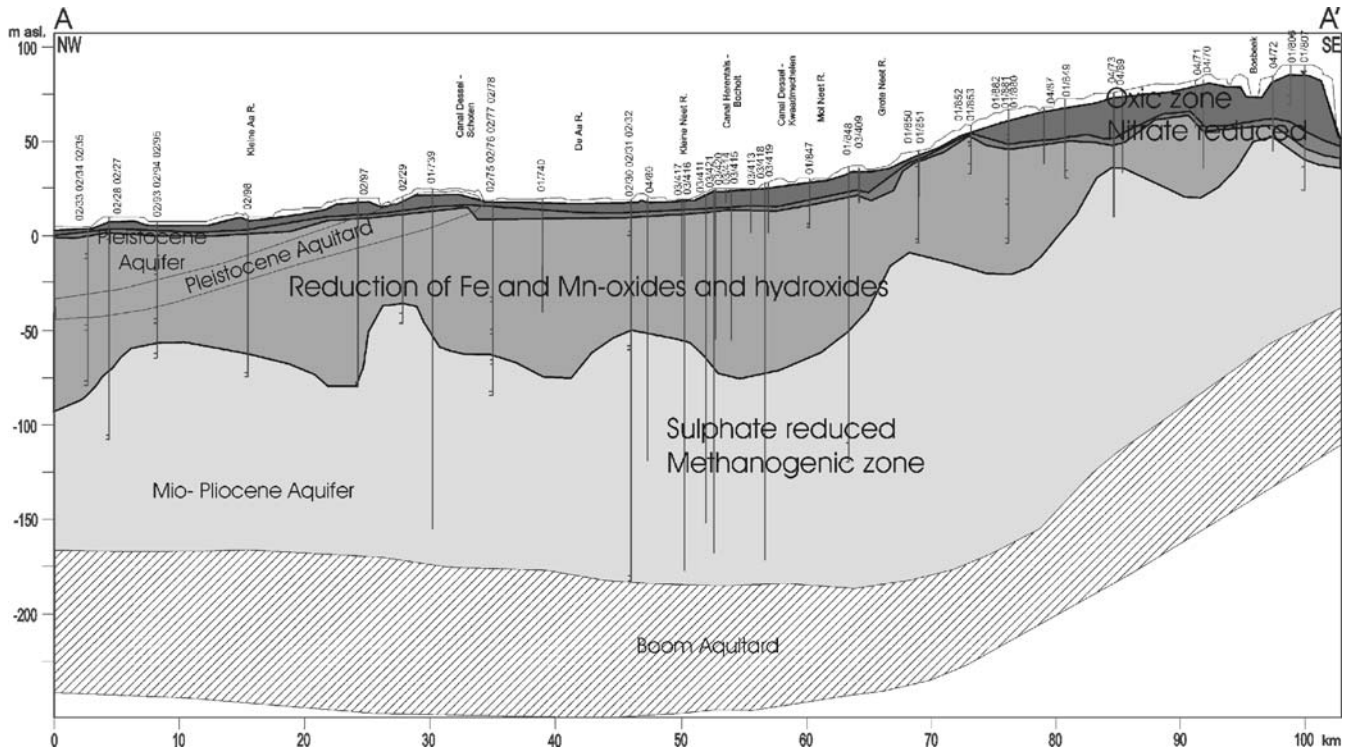


Fig. 10 Indication of redox zones on profile AA'

In brackish and salt groundwater ($\text{Cl} > 200 \text{ mg L}^{-1}$) sulphate concentrations are corrected for the percentage of sea water present. Pannatier et al. (2000) proposed a calculated relation (SO_4F) as the relative deviation of the sulphate/chloride ratio in groundwater and sea water:

$$\text{SO}_4\text{F} = \frac{\left(\frac{\text{SO}_4}{\text{Cl}}\right)_{\text{GW}} - \left(\frac{\text{SO}_4}{\text{Cl}}\right)_{\text{SW}}}{\left(\frac{\text{SO}_4}{\text{Cl}}\right)_{\text{SW}}}$$

When the SO_4F ratio is larger than -0.2 , a large sulphate content is assumed and sulphate reduction is still going on or is not yet started. In samples with an SO_4F ratio smaller than -0.2 , sulphate is reduced. Pannatier et al. (2000) propose a value of -0.2 instead of 0 to take into account small analytical errors.

In Fig. 10, the redox zones are indicated on profile AA'. In the Neogene Aquifer, dissolved oxygen and nitrate are consumed in the uppermost metres (Fig. 10). The reduction of Mn- and Fe-oxides and hydroxides brings Mn^{2+} and Fe^{2+} into the solution, while the reduction of sulphate removes iron from the solution as a result of the formation of iron sulphides. Methane was not analytically measured but Stumm and Morgan (1981) indicate that methanogenesis occurs at about the same redox potential as sulphate reduction; so it is very likely to take place in the deeper parts of the Neogene sediments. The whole redox sequence described by Berner (1981) is present in the Neogene Aquifer. The oxidation of organic

matter releases a lot of CO_2 and HCO_3^- in the groundwater system.

In Fig. 11, the measured arsenic concentration is represented versus depth together with the iron and sulphate concentration. In the uppermost metres, the arsenic concentrations are small, while an increase is observed in the region where iron increases. Pyrite oxidation by means of oxygen or nitrate reduction takes place in the shallow part of the aquifer, leading to elevated sulphate concentrations. In the shallow parts of the aquifer, no increase in Fe^{2+} is observed since the environment is not sufficiently reducing. The Fe^{2+} originating from pyrite oxidation will immediately be oxidized to Fe^{3+} , which will precipitate as iron oxides or hydroxides. Arsenic and other heavy metals incorporated in the pyrite are adsorbed to the iron oxides and hydroxides. When the environment is sufficiently reducing, the iron hydroxides are reduced and the adsorbed arsenic comes into the solution. High arsenic concentrations of more than $50 \mu\text{g L}^{-1}$ have been observed in the Neogene Aquifer. At a depth of ca. 80 m, iron and sulphate concentrations in the groundwater fall below the detection limit (Fig. 11) due to sulphate reduction and the formation of iron sulphides. Arsenic does not show a decrease at this depth and is thus not incorporated in the formed iron-sulphide minerals. Deeper in the groundwater reservoir the arsenic concentration increases even more. Dissolution of siderite can be responsible for this increase.

In the deepest parts of the Neogene Aquifer, cation exchange is taking place. Na^+ -, Mg^{2+} -, and K^+ -cations

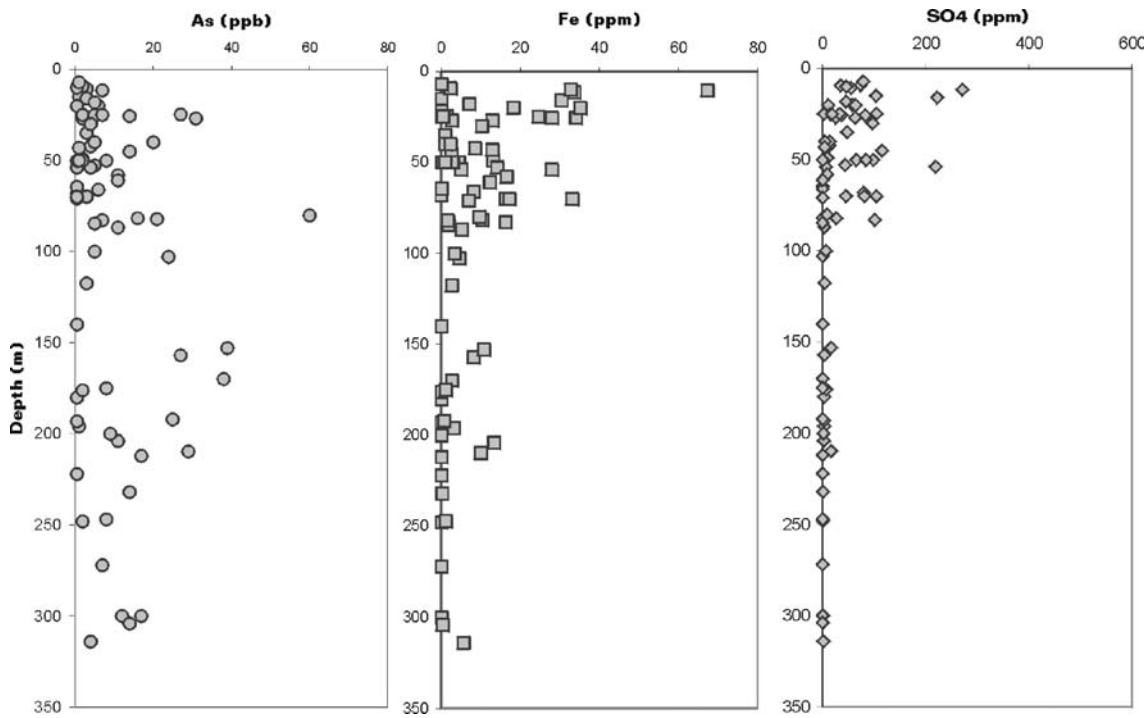


Fig. 11 Arsenic, iron and sulphate concentrations versus depth

adsorbed to the clay, are successively replaced by Ca^{2+} -ions leading to NaHCO_3 and MgHCO_3 groundwater types. High HCO_3^- concentrations can result from the depletion of Ca^{2+} due to cation exchange, which causes a second stage of calcite dissolution (Walraevens 1990). An increase in Na^+ , K^+ , and Mg^{2+} can also occur when minerals containing these ions such as feldspars dissolve (Stuyfzand 1986). Since no increase in silica concentrations is observed at this place in the aquifer system (Fig. 6), this possibility is not applicable here and cation exchange is thus responsible for the increase in Na^+ , K^+ , and Mg^{2+} .

Summary and conclusions

In this report, the hydrochemistry of the Neogene Aquifer in Belgium is presented. The Neogene Aquifer is the largest groundwater reservoir in Flanders and contains important amounts of drinking water. A large part of the aquifer is unconfined and thus vulnerable. Towards the north, a clay layer in the Pleistocene sediments makes the Neogene Aquifer semi-confined. The evolution of chemical substances in the direction of groundwater flow and in a cross-section was studied to determine the geochemical reactions that occur in the aquifer. The aquifer can be divided in two parts. The eastern part of the aquifer is decalcified, while in the western part, carbonate is still present and has an important influence on the groundwater quality. The aquifer is well flushed, leading to low mineralization of the groundwater and low pH, electrical

conductivity and HCO_3^- concentration in the shallow groundwater.

Weathering of silicate minerals, although a very slow process, causes an increase in SiO_2 and Na^+ , K^+ , Ca^{2+} and Mg^{2+} along the direction of groundwater flow. The stability of silicate minerals was checked by plotting the samples on stability diagrams and calculating the saturation index. This combined approach showed that weathering of silicates is possibly occurring in the Neogene Aquifer. The high sulphate concentrations in the shallow part of the aquifer are caused by the oxidation of pyrite by means of oxygen or nitrate. Iron from pyrite will precipitate as hydroxides in oxidizing conditions. The oxidation of organic matter occurs first by means of dissolved oxygen, followed by NO_3^- reduction, reduction of Mn-oxides and Fe-oxides and hydroxides, SO_4^{2-} reduction and methanogenesis. The whole redox sequence could be identified in the groundwater system by investigating the redox sensitive species: O_2 , NO_3^- , Mn^{2+} , $\text{Fe}^{2+/3+}$ and SO_4^{2-} . Since methane production occurs at about the same redox potential as sulphate reduction, it can be concluded that methane will probably be present in the deeper aquifer. Calcite dissolution takes place in the deeper parts and in the north where the deposits contain calcite, leading to the occurrence of CaHCO_3 groundwater types. In the deep wells, cation exchange is responsible for an increase in Na^+ , and Mg^{2+} concentrations and $\text{Mg}-$ and NaHCO_3 groundwater types are found here. Cation exchange is responsible for a second stage of calcite dissolution in the deep aquifer, causing high HCO_3^- concentrations.

Acknowledgements This study was made possible thanks to the financial support of the Special Research Fund (BOF) 01106903 of the Ghent University and the European Community Framework V project EVK1-CT1999-0006 "Baseline".

References

- Appelo CAJ, Postma D (1993) Geochemistry, ground water and pollution. Balkema, Rotterdam, Netherlands
- Berner RA (1981) A new geochemical classification of sedimentary environments. *J Sed Petrol* 51:359–365
- Camelbeeck T, Meghraoui M (1996) Large earthquakes in Northern Europe more likely than once thought. *Eos Vol* 77(42):405–409
- Coetsiers M, Van Camp M, Walraevens K (2005) Influence of the former marine conditions on groundwater quality in the neogene phreatic aquifer, flanders. In: Araguas L, Custodio E, Manzano M (eds) Groundwater and saline intrusion, selected papers from the 18th Salt Water Intrusion Meeting, Cartagena 2004, pp 499–509
- De Meuter FJ, Laga P (1976) Lithostratigraphy and biostratigraphy based on benthonic foraminifera of the Neogene deposits of northern Belgium. *Bull Belg Verenig Geol* 85(4):133–152
- Demyttenaere R, Laga P (1988) Breukken- en isohypsenkaarten van het Belgisch gedeelte van de Roerdal Slenk (Faults and isohyps maps of the Belgian part of the Roer Graben). Professional Paper 1988/4 No. 234, Belgian Geological Survey, Brussels
- Hunter KS, Wang Y, Van Cappellen P (1998) Kinetic modeling of microbially-driven redox chemistry of subsurface environments: coupling transport, microbial metabolism and geochemistry. *J Hydrol* 209:53–80
- McDonald MG, Harbaugh AW (1988) A modular three-dimensional finite-difference groundwater flow model (MODFLOW). US Geological Survey Open-File Report 83-875, US Geol Surv, Reston, VA
- Pannatier EG, Broers HP, Venema P, van Beusekom G (2000) A new process-based hydrogeochemical classification of groundwater: application to the Netherlands national monitoring system. TNO report, NITG 00-143-B, 38, NITG, Utrecht
- Parkhurst DL, Apello CAJ (1999) User's guide to PHREEQC (version 2): a computer program for speciation, reaction-path, ID-transport, and inverse geochemical calculations. US Geol Surv Water Resour Inv Rep 99-4259, US Geol Surv, Reston, VA
- Patyn J, Ledoux E, Bonne A (1989) Geohydrological research in relation to radioactive waste disposal in an argillaceous formation. *J Hydrol* 109:267–285
- Stumm W (1984) Interpretation and measurement of redox intensity in natural waters. *Schweiz Z Hydrol* 46:291–296
- Stumm W, Morgan J (1981) Aquatic chemistry: an introduction emphasizing chemical equilibria in natural waters, 2nd edn. Wiley, New York
- Stuyfzand PJ (1986) A new hydrochemical classification of water-types: principles and application to the coastal dunes aquifer system of the Netherlands. Proceedings of the 9th Salt Water Intrusion Meeting, Delft 1986, pp 641–655
- Stuyfzand PJ (1993) Hydrochemistry and hydrology of the coastal dune area of the western Netherlands. PhD Thesis, Free University Amsterdam, Netherlands
- Vandenberge N (1978) Sedimentology of the Boom Clay (Rupelian) in Belgium. Klasse der Wetenschappen, jaargang XL, No. 147, Verh. Acad. Wet., Lett. en Schone Kunsten v. België, Brussels
- Van Dyck E, Lebbe L, De Breuck W (1981) Hydrogeological, geological and ecological survey of "De Kalmthoutse Heide" and the surrounding agricultural land. Laboratory for Applied Geology and Hydrogeology, Report TGO 79/05, 94, Ghent University, Belgium
- Walraevens K (1990) Hydrogeology and hydrochemistry of the Ledo-Paniselian semi-confined aquifer in East- and West-Flanders. *Acad Analecta* 52(3):11–66
- Walraevens K, Van Camp M (2005) Advances in understanding natural groundwater quality controls in coastal aquifers. Groundwater and saline intrusion, selected papers from the 18th Salt Water Intrusion Meeting, Cartagena 2004, Spain, pp 449–463
- Walraevens K, Mahauden M, Coetsiers M (2003) Natural background concentrations of trace elements in aquifers of the Flemish Region, as a reference for the governmental sanitation policy. Proceedings of the 8th International FZK/TNO Conference on Contaminated Soil (ConSoil), Ghent 2003, pp 215–224